ACS APPLIED MATERIALS & INTERFACES

Research Article

www.acsami.org

Synthesis of Silver Nanoparticles Confined in Hierarchically Porous Monolithic Silica: A New Function in Aromatic Hydrocarbon Separations

Yang Zhu,[†] Kei Morisato,[‡] Wenyan Li,[§] Kazuyoshi Kanamori,*[,†] and Kazuki Nakanishi*[,†]

[†]Department of Chemistry, Graduate School of Science, Kyoto University, Kyoto, Japan

[‡]GL Sciences, Inc., Tokyo, Japan

[§]Department of Materials Science and Engineering, Zhejiang University, Hangzhou, P. R. China

ABSTRACT: Silver nanoparticles (Ag NPs) have been homogeneously introduced into hierarchically porous monolithic silica columns with well-defined macropores and SBA-15-type hexagonally ordered mesopores by using ethanol as the mild reductant. Within the cylindrical silica mesopores treated with aminopropyl groups as the host, monocrystalline Ag NPs and nanorods are obtained after being treated in silver nitrate/ethanol solution at room temperature for different durations of reducing time. The loading of Ag NPs in the monolith can be increased to 33 wt % by the repetitive treatment, which also led to the formation of polycrystalline Ag nanorods in the mesopores. Although the bare silica column cannot separate aromatic hydrocarbons, good separation of those molecules by noncharged Ag NPs confined in the porous structure of the monolith has been for the first time demonstrated with the Ag NP-embedded silica column. The NP-embedded monolithic silica would be a powerful separation tool for hydrocarbons with different number, position, and configuration of unsaturated bonds.

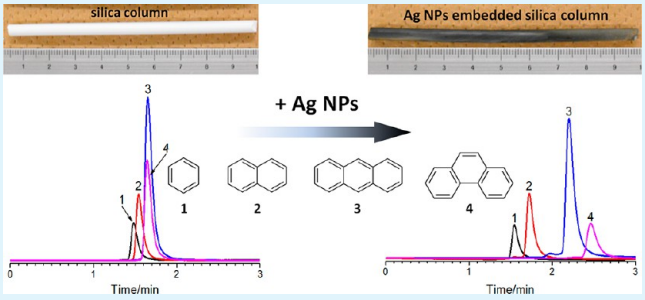

KEYWORDS: *hierarchical pores, silica monolith, silver nanoparticles, separation media, aromatic hydrocarbons*

INTRODUCTION

Mesoporous silica has long been studied as an ideal hard template and host for the formation of metallic nanostructures of different morphologies. Because of the high accessibility and high stability of the silica host, the metallic nanostructures confined in the porous structure are reasonably active and can be reused for many times, which allows the metal−silica composite to be the ideal materials for catalysis, sensors, and biomedical applications.[1−8] One of the most frequently applied mesoporous structure hosts is SBA-15-type uniform-sized cylindrical mesopores due to its simple synthetic procedure, high reproducibility, and tunable pore size,[8−12] while one of the most popular noble metals to be embedded is silver simply because it is easier to be shaped into different morphologies showing different optical and catalytic properties.[11−17] Recently Sun et al. have reported the embedment of monodispersed silver nanoparticles (Ag NPs) in SBA-15, showing unusual thermal stability at 873 K because of the confinement by the mesoporous structure.[11] Similarly, Xie et al. have reported the formations of both silver and gold nanoparticles and nanorods in SBA-15.[12] In both cases, the basic idea was to first graft the surface of the host material with amino groups which could then be turned into imine groups by the reaction with aldehydes. The high reactivity of imino groups was then used to reduce silver ions or silver amine complex into Ag NPs. Since those NPs formed in the mesopores were confined in one dimension, they tended to grow and agglomerate along the cylindrical mesopores to form Ag nanorods.

Compared to the particulate shape of silica host like SBA-15, hierarchically macro- and mesoporous silica monoliths prepared by sol−gel accompanied by phase separation are much easier to be handled, recycled, and reused, which makes it a potential candidate in the fields of separation and refinement for industrial applications.[18−22] As a possible extension of the application of silica monolith with SBA-15-type mesoporous structure, here we report an effective method for the embedment of Ag NPs into hierarchically porous monolithic silica in a mild condition. As is well-known, silver-amine complex can form when silver nitrate solution and aqueous ammonia are mixed. Instead of transferring amino groups into imino groups, silver nitrate is first added to react with amino groups to anchor silver ions at the surface of silica by forming silver-amine complex. In order to obtain Ag NPs embedded homogeneously over the whole monolith, ethanol as a mild reductant is adopted to control the rate of the redox reaction. Although the adoption of alcohol as the reductant for the production of free metallic nanostructures has long been studied,[23−28] few reports are found using alcohol as the

Received: December 18, 2012
Accepted: February 26, 2013
Published: February 26, 2013

reductant for the formation of metallic nanostructures immobilized on a porous host. At least, this is the first report on the reduction of metal ions by alcohols onto porous monolithic materials, which is advantageous in simplicity, having less post-treatment steps, and being less hazardous.

Silver ions have long been applied in the separation of lipids with different number, configuration, or position of the double bonds in the fatty acid residues since those unsaturated bonds in lipids form a weak charge transfer complex between silver ions and the π electrons of the double bonds in the unsaturated organic molecules.[29−33] The most commonly applied method for the preparation of silver-loaded HPLC columns is to attach silver ions on HPLC-grade silica gel particles by ion exchange with sulfo groups. However in its ionic state, silver is not stable for a long period of time on the silica surface, especially under the exposure of light. Therefore instead of ionic silver, Ag NPs are preferred. As is well understood, in the presence of an electron acceptor, Ag NPs could be partially charged, making it possible to form complex with an electron-donating ligands in an immobilized state. Thus ionic liquids, due to their highly charged nature, were used by Kang et al. to polarize the surface of Ag NPs.[34−36] The positively charged silver surface in an olefin transport membrane showed stable performance for the gas-phase separation of propylene/propane for over 100 h of continuous operation, showing better stability than silver in its ionic state.[34] Furthermore, simulations have been demonstrated by Pozun et al., showing the uniqueness of Ag NPs in its efficiency for the separation of olefin/paraffin because of its weak chemisorption of ethylene compared with other metals. According to their report, small NPs tend to show stronger binding over ethylene because the overall number of corners and kinks which tend to have localized electronic states and are free of steric hindrance in small NPs shall be higher than larger ones.[37]

In this report, we for the first time show the embedment of Ag NPs inside the silica monolith with well-defined macropores and SBA-15-type mesopores by the simple and mild reduction with ethanol. The performance of Ag NPs homogeneously introduced in the silica monolith for the liquid-phase separation of aromatic hydrocarbons was investigated by high-performance liquid chromatography (HPLC). The column with more than 30 wt % of silver loading showed difference in retention time large enough to discriminate benzene, naphthalene, anthracene, and phenanthrene. This reveals that Ag NPs embedded in hierarchically porous monolithic silica column contribute not only to the separation of aromatic hydrocarbons with different numbers of aromatic rings but also to that of configurational isomers with the same amount of aromatic rings. To the best of our knowledge, this is also the first experimental report about the separation of aromatic hydrocarbons by noncharged Ag NPs with a silica column by HPLC.

EXPERIMENTAL SECTION

Reagents. As the silica source, tetramethoxysilane (TMOS) was obtained from Shin-Etsu Chemical Co. Ltd. (Japan). Poly(ethylene oxide)-*block*-poly(propylene oxide)-*block*-poly(ethylene oxide) (M_w = 5800) (equivalent to Pluronic P123, BASF), (3-aminopropyl)-triethoxysilane (APTES), formaldehyde solution (37 wt % in water), silver nitrate, benzene, nitrobenzene, *o*-nitroanisole, naphthalene, anthracene, and phenanthrene were purchased from Sigma-Aldrich Co. LLC (USA). Urea and distilled water were obtained from Hayashi Pure Chemical Ind., Ltd. (Japan) and Wako Pure Chemical Ltd. (Japan), respectively. All the other reagents were of analytical grade and purchased from Kishida Chemical Co. Ltd. (Japan).

Preparation of Hierarchically Porous Silica Monolith. Preparation of hierarchically porous silica monoliths with SBA-15-type ordered mesopores is the modified version of the previous report.[20] In a typical run, 1.4 g of P123 was dissolved into 16 mL of 0.01 M acetic acid. After the complete dissolution of P123, the mixture was kept stirring for 5 min in an ice bath, followed by the addition of 1.0 g of urea. Then, 2.5 mL of TMOS was added under vigorous stirring until a clear solution was obtained. The resultant solution was then transferred to a plastic tube (inner diameter of 6 mm) with airtight lids at both ends. The plastic tube was immersed into a water bath for gelation at 60 °C followed by aging at the same temperature in an oven for 3 d. The wet gels thus obtained went through the solvent exchange process by distilled water two times and water/ethanol solution (2/1 in volume) one time for more than 12 h per each time. The solvent volume amount was at least 10 times of the volume of the gel. The gels were finally dried at room temperature for 3 d at 40 °C for 5 d. For the purpose of completely eliminating the organic species and to obtain a stable crack-free monolith, the as-dried white gel was heated with the ramp rate of 1 °C/min up to 800 °C and kept at the same temperature for 5 h. Calcination would also lead to better diffusion of Ag^+ into the mesopores as was suggested by Bessen et al.[38] After calcination, the diameter of the monolith decreased to 4.6 ± 0.2 mm (~23% total shrinkage).

Introduction of Ag NPs into Hierarchically Porous Silica Monolith. The introduction of Ag NPs into the hierarchical porous structure of silica monolith was conducted with a relatively facile and versatile method using ethanol as the reducing agent. First, 0.2 g of the silica monolith calcined at 800 °C was immersed into 20 mL of APTES/toluene (0.8/20 in volume) solution in a sealed amber test tube which was then left under 80 °C for 24 h for the modification of silica surface with aminopropyl groups. The obtained gel was then washed extensively with ethanol three times for at least 12 h per each time and was thereafter immersed into 20 mL of 50 mM ethanol solution of silver nitrate for 96 h at room temperature. Some of the samples were repeatedly processed from the aminopropyl modification step to increase the loadings of aminopropyl group and Ag NPs in the monolith. Samples subjected to different modification steps are denoted as E-*x*-*y* (*x* duration of the treatment in the $AgNO_3$/ethanol solution, *y* repetition number of the treatment starting from the modification of aminopropyl groups). The resultant black-colored gel was washed with 20 mL of ethanol three times with at least 4 h per time to completely remove free Ag^+ in the gel and dried at 60 °C for 3 d. Formaldehyde as a conventional reducing agent was employed as a comparison. In this case, instead of keeping in the ethanol solution of silver nitrate, the gel was taken out after the modification with 50 mM of ethanol solution of silver nitrate for 24 h and then immersed into 20 mL of 1 M aqueous solution of formaldehyde at room temperature for a predetermined time. The obtained gel was rinsed with 20 mL of distilled water three times with at least 4 h per time to remove free formaldehyde molecules or Ag^+ in the gel and dried at 60 °C for 3 d.

Characterization. Morphology of the fractured surfaces of the samples and its composition were characterized by a scanning electron microscope equipped with an energy-dispersive X-ray spectroscope (SEM-EDS; JSM-6060S and JED-2300, JEOL Ltd., Japan), a field-emission scanning electron microscope (FE-SEM; JSM-6700F, JEOL Ltd., Japan). The EDS spectra were taken at the cross-section of the monolith with the magnification at 40 five times, from which the average was taken to obtain the loading of silver in the monolith. Meso- and micropores were characterized by an N_2 adsorption−desorption apparatus (BELSORP-mini II, Bel Japan Inc., Japan). The samples were degassed at 200 °C under vacuum before each N_2 adsorption−desorption measurement. The BJH method was applied to adsorption branch to derive mesopore size distributions. The grafting of aminopropyl groups on the surface of silica was confirmed by thermogravimetry-differential thermal analysis (TG-DTA; Thermo plus EVO, TG 8120, Rigaku Co., Japan). The reactions were confirmed by Fourier transform infrared spectroscopy (FT-IR; IR Affinity-1, Shimadzu Co., Japan). The existence of Ag NPs in the mesopores of the silica host was confirmed by powder X-ray diffraction (XRD; RINT Ultima III, Rigaku Corp., Japan) using Cu Kα (λ = 0.154

nm) as an incident beam, UV−vis absorption spectroscopy (UV−vis) (V-670, JASCO Corp., Japan), and a transmission electron microscope (TEM; CM200UT, PHILIPS Co., Netherlands). In the UV−vis absorption measurement, 5 mg of each sample was ground and then homogeneously dispersed in 20 mL of ethanol by ultrasonic agitation for 10 min. Liquid chromatographic evaluations were carried out using an ordinary HPLC system with a pump (PU712, GL Sciences, Japan), a UV detector (MU701, GL Sciences, Japan), a data processor (EZ Chrom Elite Chromatography Data System, Agilent Technologies, USA), and a Rheodyne injector (8125, Rheodyne, USA). The system was operated in a constant-pressure mode at room temperature (~25 °C). In the separation of polycyclic aromatic hydrocarbons, 1.6 μL of benzene, 0.8 mg of naphthalene, 0.2 mg of anthracene, and 0.5 mg of phenanthrene were dissolved in 1 mL of *n*-hexane as a standard sample. The injection volume was 1 μL in each case.

RESULTS AND DISCUSSION

Silica Monolith Used As the Host. Figure 1 shows the micrometer-scale morphology of the crack-free silica monolith

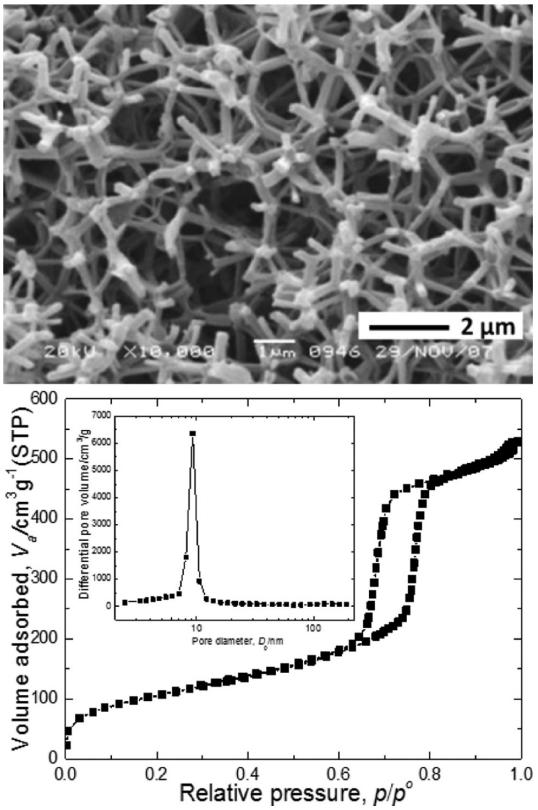

Figure 1. SEM image and N_2 adsorption−desorption isotherm (inset is the mesopore size distribution obtained by BJH method using adsorption branch) of the silica monolith calcined at 800 °C.

after calcination at 800 °C. Compared to the previous report, crack-free monoliths are achieved by employing the one-pot acid−base two-step reaction catalyzed by acetic acid and hydrolysis product (ammonia) of urea, respectively. The slow hydrolysis of urea into carbon dioxide and ammonia at 60 °C leads to the base-catalyzed polycondensation allows forming the more densely condensed network with high mechanical strength. The calcined silica monolith, which will be further used as the host for Ag NPs, consists of ca. 1.5 μm macropores and ca. 9.2 nm uniform-sized cylindrical mesopores in ca. 200 nm-thick rod-like skeletons as can be recognized from the SEM image and nitrogen isotherm with type-IV hysteresis shown in Figure 1. The SBA-15-type ordered mesopores are confirmed in TEM images shown later. The specific surface area of the silica monolith reaches 393 m^2 g^{-1}. The characteristic structure has been formed through the combination of phase separation and SBA-15-type structural directing by surfactant micelles as reported in detail previously.[20]

The modification of host monolith with aminopropyl groups is achieved by the reaction of APTES and silanol groups on the silica surface. From TG-DTA results in Figure 2, a resolved

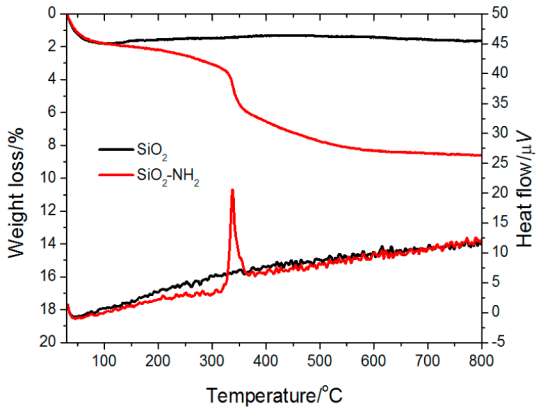

Figure 2. TG-DTA curves of silica monolith calcined at 800 °C (black curve) and aminopropyl-modified silica monolith (red curve).

exothermic peak between 300 and 350 °C due to the pyrolysis of aminopropyl groups on the silica surface can be observed. Further weight loss can be found as temperature rises from 350 to 600 °C which can be attributed to the oxidative decomposition of carbonaceous products derived from aminopropyl groups.

Comparison between Reduction by Formaldehyde and Ethanol. Figure 3 shows the UV−vis spectra of Ag NPs formed in the silica monolith after the addition of formaldehyde (parts A and B) and ethanol (part C), respectively. Much higher reactivity of formaldehyde in the reduction of Ag^+ on the silica surface than that of ethanol is revealed as a larger amount of Ag NPs was formed in much shorter time in the case of formaldehyde. As is shown in Figure 3A, the intensity of the absorption band at around 420 nm due to the transverse plasmon resonance of Ag NPs increased in the first 30 min, where the loading of Ag NPs in the monolith reached a maximum. Then, a distinct decrease of the intensity appeared as time elapsed, indicating obvious leaking of Ag NPs from the monolith (Figure 3B). After the monolith was immersed into the formaldehyde solution, diffusion of formaldehyde through the porous structure into the monolith started. The Ag^+ at the macropore surface of the monolith and the free Ag^+ in the solution were first reduced to Ag NPs especially in the outer parts of the monolith. Before immobilization by aminopropyl groups on the silica surface or confined by the mesoporous structure as mentioned later, agglomeration happened in the first place and the particles grew too large to be immobilized or confined. These large particles diffuse away into the bulk solution, leaving the smaller NPs which can be confirmed by a blue shift of the absorption band from 436 nm (30 min) to 425 nm (1 h). Also, because of the leakage of the large particles in the monolith as described above, the outer part of the monolith showed a relatively lighter color than the inner part (Figures 4A and C).

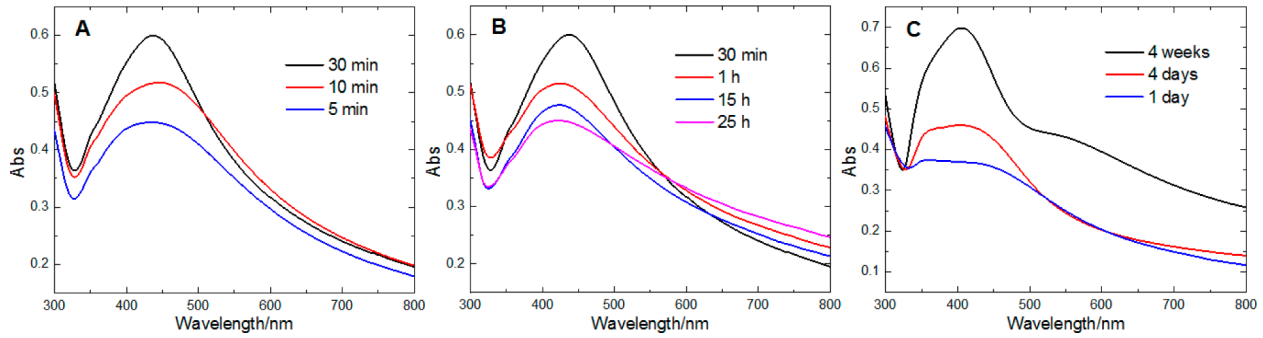

Figure 3. Time evolution of UV−vis spectra of Ag NPs in the silica monolith by the reduction with formaldehyde (A and B) and ethanol (C).

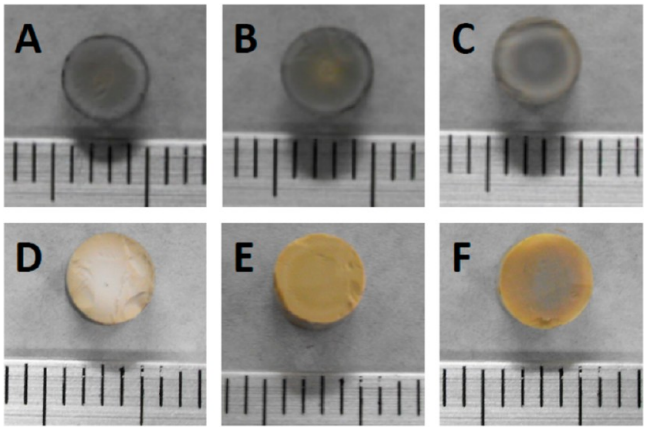

Figure 4. Photographs of the cross-section of silica monoliths after the introduction of Ag NPs with formaldehyde for 5 min (A), 30 min (B), 25 h (C) and with ethanol for 1 day (D), 4 days (E), and 4 weeks (F) as the reductants.

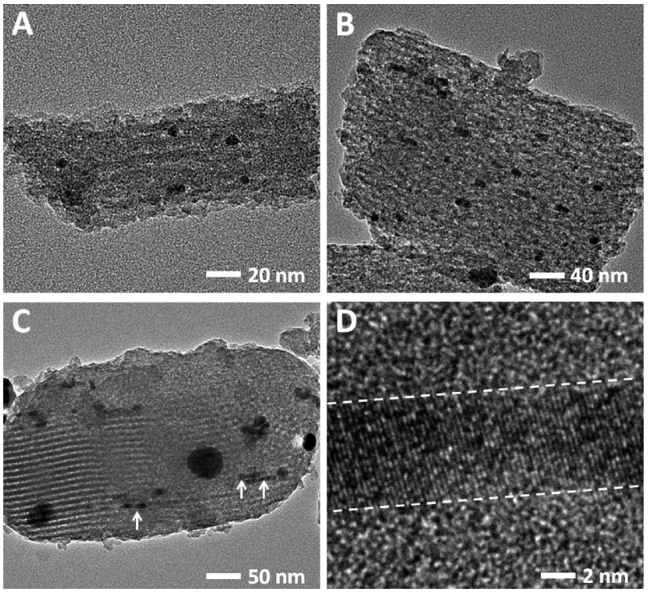

Figure 5. TEM images of silica monoliths treated with 50 mM $AgNO_3$ ethanol solution for 1 day (A), 4 days (B), 4 weeks (C), and the magnification of C at the rod part pointed out by arrows (D).

On the other hand, in the case of ethanol, the increase of Ag NPs in the monolith in proportion to the treating time was observed in the increased absorptions around 400 nm due to the transverse plasmon resonance of Ag NPs and around 350 nm due to the formation of plate-like Ag particles.[39] Besides, the shoulder around 570 nm due to the longitudinal plasmon resonance was observed in the spectrum of the sample treated for 4 weeks, suggesting the formation of Ag monocrystalline nanorods in the silica monolith giving out the bluish color in the central part of the monolith as shown in Figure 4F.[12,39] As the reduction ability of ethanol is considerably lower compared to formaldehyde, most of the Ag^+ in the solution stayed stable for longer time, which allowed their diffusion into the mesopores. Since most of the surface area inside the templated skeletons is contributed by the mesopores, most of the Ag^+ was then immobilized on the mesopore surfaces by the interaction between Ag^+ and aminopropyl groups, followed by the mild reduction by ethanol. As treating time becomes longer, more particles are formed as can be seen from Figures 5A−C. Without spatial confinement, those immobilized at the external surface of the rod-like skeletons grew larger into the plate-like particles (Figure 5C) while most of the particles were formed in the mesopores in the first place and grew within the confined space. As a result, some of the particles possibly grew into monocrystalline nanorods within the cylindrical mesopores as reaction time is increased (Figures 5C and D). If the effect of diffusion is negligible, the reduction should take place at the same time over the whole monolith, making it possible to obtain a more homogeneous distribution of Ag NPs by using ethanol as the mild reductant (Figures 4E and F). However compared with the milder way of reduction by ethanol, in the case of formaldehyde as the reductant, the reduction occurred in a more aggressive manner regardless the position of amino groups, which may cause crystallization in any place rather than epitaxial growth observed in ethanol reduction, thus resulting in the formation of mainly big Ag particles outside the mesopores.

Increase of Ag Loading by Repeated Treatment. Repeated treatment has been frequently used to increase the amount of embedded substances in porous systems or strengthen the porous structure.[40−43] We can assume that most of the available aminopropyl groups on the surface of silica monolith were blocked by Ag^+ due to their interaction after the treatment by silver nitrate solution, since the excessive amount of $AgNO_3$ solution was added for every sample. In order to increase the loading of Ag NPs, the repetition of the treatment was conducted from the modification step by aminopropyl groups to increase the loading of aminopropyl groups on the surface of the monolith. Figure 6 shows the TG curves of samples treated for different repetition times. Instead of one-step weight loss shown in Figure 2 for the silica monolith modified with aminopropyl groups, two steps of weight loss appear in the TG curves of the samples treated repeatedly. The weight losses from 300 to 600 °C which could

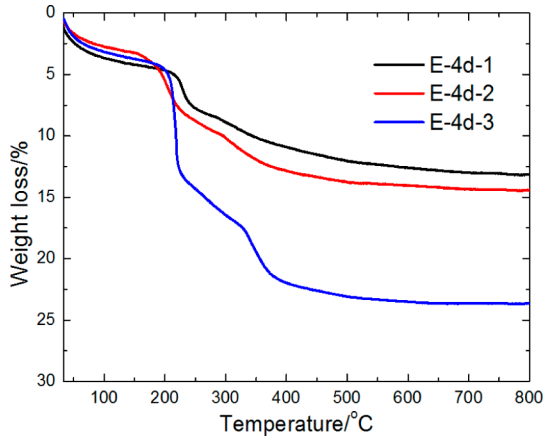

Figure 6. TG curves of E-4d-1, E-4d-2, and E-4d-3 samples.

be attributed to the pyrolysis of aminopropyl groups were 3.7, 3.9, and 7.1 wt % for one, two, and three times, which correspond to the surface coverage of aminopropyl groups on silica to be 0.64, 0.67, and 1.2 mmol/g, respectively. Since the silica monolith was precalcined, the weight loss from the elimination of silanol groups from 300 to 600 °C is negligible. Thus the loading of aminopropyl groups increased with increasing number of repetition. Meanwhile, the weight loss at around 200 °C can be attributed to the oxidation of $-NH_3^+NO_3^-$ ion pairs on the silica surface, which is also confirmed by FT-IR spectra. From the FT-IR spectra, a sharp absorption peak at 1385 cm^{-1} due to ionic nitrate attached on the surface as $-NH_3^+NO_3^-$ ion pairs could be observed (Figure 7).[44−46] As the treatment was repeated, more silver nitrate was

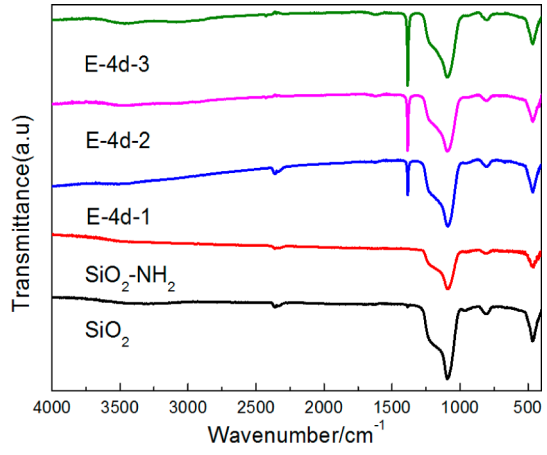

Figure 7. FT-IR spectra of pure silica, aminopropyl-modified silica monolith, and silver-loaded monoliths E-4d-1, E-4d-2, and E-4d-3.

reacted on the silica surface, giving rise to larger weight loss in the TG curves. In parallel, stronger absorption by the ion pair was recognized in the FT-IR spectra compared to that of Si−O−Si bonding at around 1200 cm^{-1} presumably due to the increased introduction of amino groups on silica. Figure 8A shows the increase of the intensity of the XRD profiles of Ag NP-loaded silica monoliths treated for different repetition times, which distinctly demonstrates the fact that the loading of Ag NPs in the silica monolith increases with the repetition of treatments. Similar conclusion can be drawn from the UV−vis spectra shown in Figure 8B, which represents the increasing absorption intensity with increasing number of repetition.

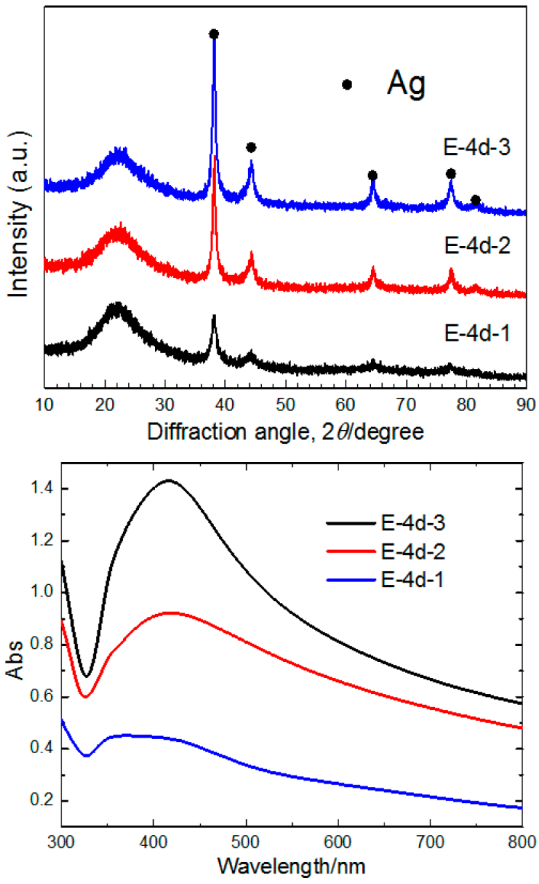

Figure 8. XRD patterns and UV−vis spectra of E-4d-1, E-4d-2, and E-4d-3.

Detailed average loading of silver in the monoliths is calculated to be 5.3 ± 0.8, 20.9 ± 0.7, and 33.3 ± 0.7 wt % from the results of EDS for the samples treated one, two, and three times, respectively, showing the increase of Ag loading in the monolith simply by repeating the experiment. Compared to Figure 4B (E-4d-1), more Ag NPs with their size ranging from 5 to 10 nm can be found in Figure 9A (E-4d-2), and in the sample treated repeatedly 3 times (E-4d-3, Figure 9B) again Ag nanorod-like crystals are observed. However, there is no evident absorption at 550 nm found in the UV−vis spectra simply because the rod-like particles are the collection of small Ag NPs with their size about 1−2 nm which are closely located to each other as shown in Figure 9C. Some of the NPs are attached to form polycrystalline rods or are separated with the voids of 1−2 nm. As the treatment is repeated from the modification with aminopropyl groups, because of the affinity between aminopropyl groups and Ag NPs, those APTES molecules added for the following treatment are attracted by Ag NPs and are thus preferentially grafted on the silica surface near the NPs. Since most of those already grafted aminopropyl groups are either covered by already formed nanoparticles or reacted with HNO_3 to form $-NH_3^+NO_3^-$ ion pairs, the free Ag^+ in the solution will prefer to be immobilized by the newly grafted aminopropyl groups which will be then in situ reduced by ethanol and grow into small NPs just near the original Ag NPs in the mesopores. The more the treatment is repeated, the more these closely located or even attached small NPs will form. Because the space in the mesopores becomes more and more limited as more NPs are formed, some of the mesopores

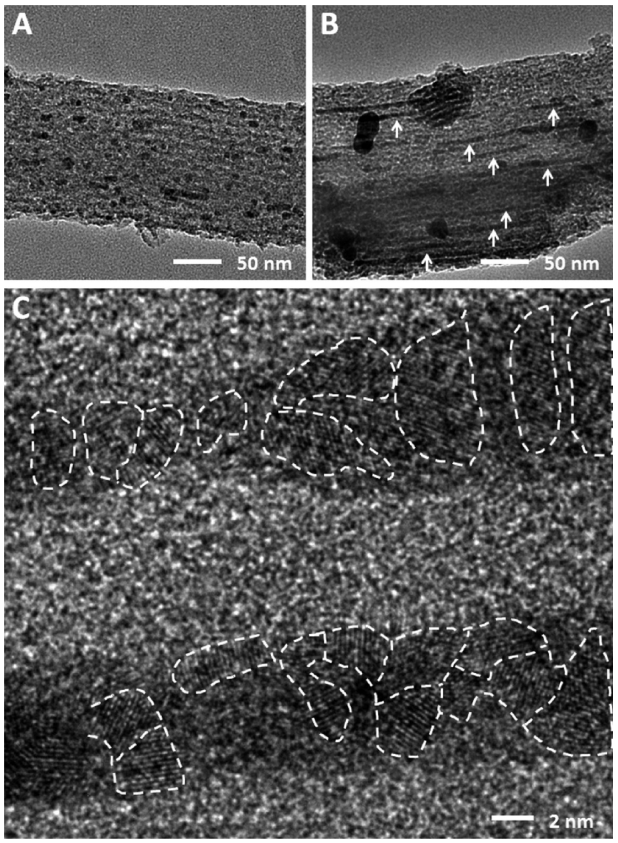

Figure 9. TEM images of E-4d-2 (A), E-4d-3 (B), and the magnification of B at the rod part pointed out by the arrows (C).

are blocked and the growth of those NPs may stop due to the shortage of free Ag^+, leaving voids among those nanoparticles, altogether of which appeared to be long Ag nanorods at the lower magnification under TEM observation.

Performance of HPLC Column for Aromatic Hydrocarbon Separations. The separation performance of the host silica monolithic column is shown in Figure 10, in which strong retention of polar aromatic compounds is demonstrated in the normal-phase separation mode. Detailed parameters are shown in Table 1. The theoretical plate number for retained analyte *o*-nitroanisole is 37 000 m^{-1}, and the separation factor between nitrobenzene and *o*-nitroanisole is 3.29, showing good performance in the separation of compounds with different polarity by the host silica monolithic column. The separation results show the homogeneity in the pore structure of the host silica monolith, which will be a good candidate for the introduction of Ag NPs into the monolith.

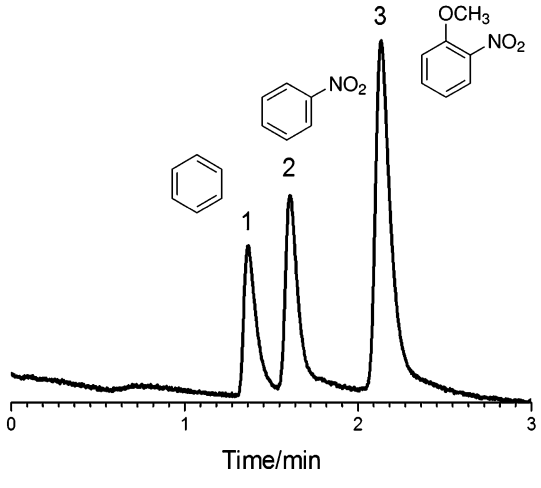

Figure 10. Chromatogram of benzene (1), nitrobenzene (2), and *o*-nitroanisole (3) obtained by the host silica column. Conditions: mobile phase hexane/ethanol = 98/2 (v/v), flow rate 1.0 mL/min, detector UV 254 nm, pressure 1.8 MPa, column length 83 mm.

Table 1. Calculated Values of Retention Factor, Plate Number, Peak Symmetry, and Separation Factor for Polar Compounds Separated by the Host Silica Monolithic Column

analytes	k^a	N^b /m^{-1}	S^c	α^d
benzene	0	22000	1.88	
nitrobenzene	0.17	31000	1.85	3.29
o-nitroanisole	0.56	37000	1.64	

[a]Retention factor calculated as $(t_R - t_b)/t_b$, where t_R is the elution time of nitrobenzene or *o*-nitroanisole and t_b is the elution time of benzene. [b]Theoretical plate number calculated as $5.54(t_R/w_{0.5})$, where t_R and $w_{0.5}$ are the retention time and peak width at half height. [c]Peak symmetry calculated as the ratio between the bandwidths before and after the peak at 10% height. [d]Separation factor calculated as $k_{\text{nitrobenzene}}/k_{\text{o-nitroanisole}}$.

In most cases, the separation performance of HPLC column partly depends on the homogeneity of the structure and/or the distribution of the retention site over the whole column. Because of its poor homogeneity of the distribution of Ag NPs formed using formaldehyde as a reductant, ethanol was preferred here to prepare the more homogeneous column for better HPLC separation. Figure 11A shows the appearance of the Ag NPs-embedded silica column treated one time, which gave a black color due to the high concentration of Ag NPs per unit volume, in comparison with an unloaded silica column. Only small differences in retention time among four different polyaromatic compounds (benzene, naphthalene, anthracene,

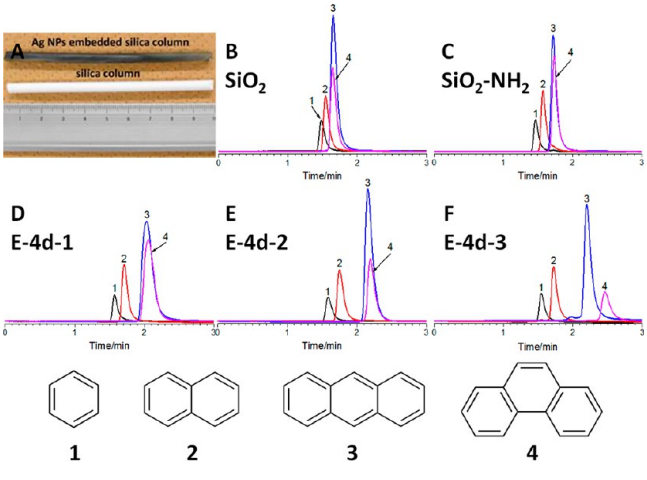

Figure 11. Appearance of the rod-shaped monolithic silica column and Ag NP-embedded silica column (A) and chromatograms of benzene (1), naphthalene (2), anthracene (3), and phenanthrene (4) obtained using the columns with different amounts of Ag NP-embeddings: (B) SiO_2, (C) SiO_2–NH_2, (D) E-4d-1, (E) E-4d-2, (F) E-4d-3. Chromatorgraphic conditions: mobile phase 0.2% acetonitrile/hexane, flow rate 1.0 mL/min, detector UV254 nm, pressure 1.5 MPa, column length 83 mm.

and phenanthrene) were observed in the cases of pure silica monolithic column and aminopropyl-modified monolithic silica column as can be seen in Figures 11B and C possibly due to their different molecular size. The comparison among Figures 11B–D reveals, however, that the retention of all the four compounds becomes stronger with increasing loading of Ag NPs to the silica monolith. The more unsaturated bonds the compound has, the stronger the interaction between the material and compound becomes and the stronger the retention of the compound is showing the capability of the Ag NP-loaded silica monolith in the separation of aromatic hydrocarbons with different number of unsaturated bonds. Since the $-NH_3^+NO_3^-$ ion pairs on the silica surface do not have affinity toward unsaturated bonds, the increased retention factors can only be attributed to the presence of Ag NPs in the monolith, which demonstrates the capability of noncharged Ag NPs for the separation of aromatic hydrocarbons. Although nanoparticles are electrically neutral, it is well-known that they show high physicochemical activity due to their small size and high surface area. According to the simulation by Pozun et al.,[37] Ag NPs tend to have affinity toward electron-rich unsaturated bonds on their surface, because of the delocalization of charge in Ag NPs. With increasing loaded amount of Ag NPs, the accessible surface area of Ag NPs becomes higher, which in total makes the retention of the aromatic hydrocarbons stronger. This is in accordance with the experimental results we have obtained. The relatively small plate number obtained in the peaks in Figure 11D may be attributed to the rather inhomogeneous distribution of Ag NPs within the monolith. Also, the broader peak widths at lower Ag NPs loadings are attributed to the increased inhomogeneity of distribution of Ag NPs over the monolith. As can further be seen in Figures 11E and F, with the increase of Ag NPs loading in the monolith, sharper peaks and even longer retention time for anthracene and phenanthrene were observed (see also Table 2 for obtained parameters), suggesting improved homogeneity of the distribution of Ag NPs in the monolith. The effective separation of compounds with different numbers of unsaturated bonds (benzene, naphthalene, and anthracene) and compounds with the same number of unsaturated bonds but different configuration (anthracene and phenanthrene) is achieved after the monolith was treated repeatedly from the modification of aminopropyl groups three times giving the theoretical plate number of about 30 000 m^{-1} for retained analyte anthracene (Table 2).

Table 2. Calculated Values of Retention Factor, Plate Number, Peak Symmetry, and Separation Factor for Aromatic Hydrocarbons Separated by the Ag NP-Embedded Silica Monolithic Columns

	anthracene			phenanthrene			
sample	k_a[a]	N_a[b] /m^{-1}	S_a[c]	k_p	N_p/m^{-1}	S_p	α[d]
E-4d-1	0.29	9900	1.49	0.31	11000	1.40	1.07
E-4d-2	0.36	24000	1.71	0.38	28000	1.68	1.06
E-4d-3	0.43	30000	1.75	0.59	24000	1.74	1.37

[a]Retention factor calculated as $(t_R - t_b)/t_b$, where t_R is the elution time of anthracene or phenanphrene and t_b is the elution time of benzene. [b]Theoretical plate number calculated as $5.54(t_R/w_{0.5})$, where t_R and $w_{0.5}$ are the retention time and peak width at half height. [c]Peak symmetry calculated as the ratio between the bandwidths before and after the peak at 10% height. [d]Separation factor calculated as k_a/k_p.

Since the difference in plate number between columns prepared with the host silica monolith and those with the highest Ag NPs loading is relatively small, the Ag NP loading does not significantly reduce the original column performance. The overall plate number must be improved by the optimization of host silica structure by changing mesopore/skeleton size and porosity. On the basis of these established methods of immobilizing metal NPs onto silica surfaces, other noble metals such as Au and Pt will easily be loaded onto the silica monolith. As has been recently shown for the effective use of Au-loaded polymer monoliths for peptides separations,[47−49] various separation functionality utilizing metal NPs will further be extensively exploited also with monolithic silica columns because of the much better separation of small molecules.

CONCLUSIONS

Silver nanoparticles have been successfully introduced into the hierarchically porous monolithic silica column with well-defined macropores and SBA-15-type hexagonally ordered mesopores. Better homogeneity of the distribution of the NPs in the monolith is obtained in the case of ethanol rather than formaldehyde used as the reductant. With the cylindrical mesopores as the host, monocrystalline Ag nanorods are obtained after being extensively treated in silver nitrate/ethanol solution. The loading of Ag NPs in the monolith was further increased by the repetition of the grafting of aminopropyl groups, introducing and reducing silver nitrate in the monolith, which also led to the formation of polycrystalline Ag nanorods in the mesopores. The Ag NPs-embedded silica columns show good separation of aromatic hydrocarbons by noncharged Ag NPs confined in the porous structure of the monolith. There is also high possibility for separations of various hydrocarbons bearing different number, type and configurations of unsaturated bonds. In addition, the present reduction technique can further be extended to the preparation of various metal NPs-embedded monolithic silica materials for applications such as to separation, adsorption, catalyst, and their combinatorial devices.

AUTHOR INFORMATION

Corresponding Author

*Phone/Fax: +81-75-753-7673. E-mail: kamori@kuchem.kyoto-u.ac.jp (K.K.). Phone/Fax: +81-75-753-2925, E-mail: kazuki@kuchem.kyoto-u.ac.jp (K.N.).

Notes

The authors declare no competing financial interest.

ACKNOWLEDGMENTS

This work was partly supported by Advanced Low Carbon Technology Research and Development Program of Japan Science and Technology Agency (JST).

REFERENCES

(1) White, R. J.; Luque, R.; Budarin, V. L.; Clark, J. H.; Macquarrie, D. J. *Chem. Soc. Rev.* **2009**, *38*, 481.
(2) Jones, M. R.; Osberg, K. D.; Macfarlane, R. J.; Langille, M. R.; Mirkin, C. A. *Chem. Rev.* **2011**, *111*, 3736.
(3) Yang, P. P.; Gai, S. L.; Lin, J. *Chem. Rev. Soc.* **2012**, *41*, 3679.
(4) Li, Z. X.; Barnes, J. C.; Bosoy, A.; Stoddart, J. F.; Zink, J. I. *Chem. Rev. Soc.* **2012**, *41*, 2590.
(5) Tang, F. Q.; Li, L. L.; Chen, D. *Adv. Mater.* **2012**, *24*, 1504.
(6) Crowley, T. A.; Ziegler, K. J.; Lyons, D. M.; Erts, D.; Olin, H.; Morris, M. A.; Holmes, J. D. *Chem. Mater.* **2003**, *15*, 3518.
(7) Han, Y. J.; Kim, J. M.; Stucky, G. D. *Chem. Mater.* **2000**, *12*, 2068.

(8) Ariga, K.; Vinu, A.; Yamauchi, Y.; Ji, Q. M.; Hill, J. P. *Bull. Chem. Soc. Jpn.* **2012**, *85*, 1.
(9) Shakeri, M.; Tai, C.; Göthelid, E.; Oscarsson, S.; Bäckvall, J. E. *Chem.—Eur. J.* **2011**, *17*, 13269.
(10) Fattori, N.; Maroneze, C. M.; Costa, L. P.; da; Strauss, M.; Sigoli, F. A.; Mazali, I. O.; Gushikem, Y. *Langmuir* **2012**, *28*, 10281.
(11) Sun, J. M.; Ma, D.; Zhang, H.; Liu, X. M.; Han, X. W.; Bao, X. H.; Weinberg, G.; Pfänder, N.; Su, D. S. *J. Am. Chem. Soc.* **2006**, *128*, 15756.
(12) Xie, Y. W.; Quinlivan, S.; Asefa, T. *J. Phys. Chem. C* **2008**, *112*, 9996.
(13) Sun, Y. G.; Xia, Y. N. *Science* **2002**, *298*, 2176.
(14) Liz-Marzán, L. M. *Langmuir* **2006**, *22*, 32.
(15) Besson, S.; Gacoin, T.; Ricolleau, C.; Boilot, J. P. *Chem. Commun.* **2003**, *3*, 360.
(16) Liong, M.; France, B.; Bradley, K. A.; Zink, J. I. *Adv. Mater.* **2009**, *21*, 1684.
(17) Hornebecq, V.; Antonietti, M.; Cardinal, T.; Treguer-Delapierre, M. *Chem. Mater.* **2003**, *15*, 1993.
(18) Nakanishi, K. *J. Porous Mater.* **1997**, *4*, 67.
(19) Tanaka, N.; Kobayashi, H.; Ishizuka, N.; Minakuchi, H.; Nakanishi, K.; Hosoya, K.; Ikegami, T. *J. Chromatogr. A* **2002**, *965*, 35.
(20) Amatani, T.; Nakanishi, K.; Hirao, K.; Kodaira, T. *Chem. Mater.* **2005**, *17*, 2114.
(21) Nakanishi, K.; Tanaka, N. *Acc. Chem. Res.* **2007**, *40*, 863.
(22) Nakanishi, K.; Amatani, T.; Yano, S.; Kodaira, T. *Chem. Mater.* **2008**, *20*, 1108.
(23) Hirai, H.; Nakao, Y.; Toshima, N. *Chem. Lett.* **1976**, *5*, 905.
(24) Tokonami, S.; Morita, N.; Takahashi, K.; Toshima, N. *J. Phys. Chem. C* **2010**, *114*, 10336.
(25) Pastoriza-Santos, I.; Liz-Marzán, L. M. *Pure Appl. Chem.* **2000**, *72*, 83.
(26) Pal, A.; Shah, S.; Devi, S. *Mater. Chem. Phys.* **2009**, *114*, 530.
(27) Hah, H. J.; Koo, S. M. *J. Sol-Gel Sci. Tech.* **2003**, *26*, 467.
(28) Kim, J. S. *J. Ind. Eng. Chem.* **2007**, *13*, 566.
(29) Morris, L. J. *J. Lipid Res.* **1966**, *7*, 717.
(30) Damyanova, B. N. *J. Chromatogr. A* **2009**, *1216*, 1815.
(31) Lisa, M.; Velínská, H.; Holčapek, M. *Anal. Chem.* **2009**, *81*, 3903.
(32) Rodríguez-Alcalá, L. M.; Braga, T.; Malcata, F. X.; Gomes, A.; Fontecha, J. *Food. Chem.* **2011**, *125*, 1373.
(33) Kuhnt, K.; Degen, C.; Jahreis, G. *J. Chromatogr. B* **2010**, *878*, 88.
(34) Kang, Y. S.; Kang, S. W.; Kim, H.; Kim, J. H.; Won, J.; Kim, C. K.; Char, K. *Adv. Mater.* **2007**, *19*, 475.
(35) Kang, S. W.; Char, K.; Kang, Y. S. *Chem. Mater.* **2008**, *20*, 1308.
(36) Kang, S. W.; Hong, J.; Kim, J. H.; Kang, Y. S. *Macromolecular Res.* **2011**, *19*, 413.
(37) Pozun, Z. D.; Tran, K.; Shi, A.; Smith, R. H.; Henkelman, G. *J. Phys. Chem. C* **2011**, *115*, 1811.
(38) Besson, S.; Gacoin, T.; Ricolleau, C.; Boilot, J. *Chem. Commun.* **2003**, 360.
(39) Sun, Y. G.; Gates, B.; Mayers, B.; Xia, Y. N. *Nano Lett.* **2002**, *2*, 165.
(40) Ma, J.; Wang, C.; Peng, K. W. *Biomaterials* **2003**, *24*, 3505.
(41) Kubo, M.; Chaikittisilp, W.; Okubo, T. *Chem. Mater.* **2008**, *20*, 2887.
(42) Liang, Z.; Susha, A. S.; Yu, A.; Caruso, F. *Adv. Mater.* **2003**, *15*, 1849.
(43) Qian, J. M.; Jin, Z. H. *J. Eur. Ceram. Soc.* **2006**, *26*, 1311.
(44) Nakamoto, K. *Infrared and Raman Spectra of Inorganic and Coordination Compounds*, 6th ed.; Wiley-Interscience: New York, 2009.
(45) Linker, R.; Shmulevich, I.; Kenny, A.; Shaviv, A. *Chemosphere* **2005**, *61*, 652.
(46) Shimizu, K.; Kawabata, H.; Satsuma, A.; Hottori, T. *J. Phys. Chem. B* **1999**, *103*, 5240.
(47) Xu, Y.; Cao, Q.; Svec, F.; Fréchet, J. M. J. *Anal. Chem.* **2010**, *82*, 3352.
(48) Cao, Q.; Xu, Y.; Liu, F.; Svec, F.; Fréchet, J. M. J. *Anal. Chem.* **2010**, *82*, 7416.
(49) Lv, Y. Q.; Lin, Z. X.; Svec, F. *Anal. Chem.* **2012**, *84*, 8457.